

# Assessment of Hypoxia in Experimental Mice Tumours by [<sup>18</sup>F]Fluoromisonidazole PET and pO<sub>2</sub> Electrode Measurements

## *Influence of Tumour Volume and Carbogen Breathing*

Lise Bentzen, Susanne Keiding, Michael R. Horsman, Tove Grönroos, Søren B. Hansen and Jens Overgaard

From the Danish Cancer Society, Department of Experimental Clinical Oncology (L. Bentzen, M.R. Horsman, J. Overgaard), PET Centre (S. Keiding, S.B. Hansen), Department of Medicine V (S. Keiding), Aarhus University Hospital, Aarhus, Denmark and Turku PET Centre (T. Grönroos), Turku, Finland

Correspondence to: Lise Bentzen, Danish Cancer Society, Department of Experimental Clinical Oncology, Aarhus University Hospital, Noerrebrogade 44, Bld. 5, DK-8000 Aarhus C, Denmark. Tel: + 45 8949 2620. Fax: + 45 8619 7109. E-mail: lise@oncology.dk

---

Acta Oncologica Vol. 41, No. 3, pp. 304–312, 2002

The aim of this study was to compare a non-invasive <sup>18</sup>F-fluoromisonidazole ([<sup>18</sup>F]FMISO) PET assessment of tumour hypoxia with invasive Eppendorf pO<sub>2</sub> measurements in 150–1500 mm<sup>3</sup> C3H mammary carcinomas transplanted on the back of CDF1 mice. The tumour-bearing mice breathed either carbogen gas (95% oxygen, 5% CO<sub>2</sub>) or normal air during both examinations. Additional autoradiography was performed in separate tumours treated similarly. The PET [<sup>18</sup>F]FMISO examination significantly discriminated between tumours of carbogen and air-breathing mice. For the pO<sub>2</sub> measurements, there was a significantly lower percentage of measurements below 2.5 mmHg for carbogen-treated mice compared with air-breathing mice. However, no direct correlation between the methods was seen. A correlation was found between tumour volume and Eppendorf estimates of tumour hypoxia for the animals breathing normal air, but no correlation was found between the PET endpoint and tumour volume. This may be due to low pO<sub>2</sub> measurements obtained in necrotic tissue. Autoradiography confirmed lower [<sup>18</sup>F]FMISO uptake in tumours of carbogen-breathing animals compared with air-breathing animals, and demonstrated the heterogeneity of the tracer uptake in small compared with larger tumours.

Received 13 August 2001

Accepted 29 January 2002

---

Some solid tumours outgrow their vasculature and as a result of insufficient blood supply, hypoxia and necrosis will develop. This hypoxia may create resistance to cancer therapy (1–4) and seems to be of prognostic importance for malignant progression of the tumour (5–8). Assessment of tumour oxygenation is therefore likely to be important for the understanding of treatment effect in tumours.

Oxygen partial pressure (pO<sub>2</sub>) can be measured in tumour tissue with oxygen-sensitive electrodes, and a prognostic relationship between tumour pO<sub>2</sub> distribution and treatment outcome for patients with cervical tumours, head and neck tumours and soft tissue sarcomas has been shown (9–12). The oxygen electrode method has obvious limitations in the clinical setting due to accessibility of the tumours. Moreover, the oxygen electrode method suffers from possible measurements in non-viable tissue (13).

Tumour hypoxia can also be assessed using the binding of hypoxia markers. Nitroimidazoles were found to be reduced under hypoxic conditions and bound to cellular macromolecules (14, 15), and this binding was shown to correlate with radiobiological hypoxia determined by a clonogenic cell survival assay (16). Binding of the hypoxia marker can be visualized by immunohistochemistry or autoradiography examination of biopsy tissue; e.g. <sup>3</sup>H-misonidazole was found to bind to hypoxic tissue in spheroids and certain tumours (17, 18). Non-invasive imaging of hypoxia in tumours in the intact organism by positron emission tomography (PET) is under continued development and preliminary clinical studies reported binding of a fluorinated misonidazole in human solid tumours (19–21). In a recent study we established a non-invasive method to assess hypoxia in experimental mouse mammary carcinomas by PET scanning using <sup>18</sup>F-fluoromisonidazole

[<sup>18</sup>F]FMISO). With this method we were able to discriminate between tumours growing on mice breathing carbogen gas (95% oxygen and 5% CO<sub>2</sub>) as compared with normal air (21% oxygen) (22).

Studies to examine the relationship between the invasive pO<sub>2</sub> measurements and the binding of hypoxia markers have been performed. Raleigh et al. (23) found that binding of pimonidazole in experimental mice tumours (as determined by immunohistochemistry) correlated well with pO<sub>2</sub> measurements, whereas this was not the case in two recent studies (24, 25) using the 2-nitroimidazole EF5 in rodent tumours and human squamous cell carcinomas, respectively. In the study by Piert et al. (26) on hypoxia in the pig liver, a correlation between PET-assessed uptake of fluoromisonidazole and Eppendorf electrode measurements was shown, thus indicating that the binding of fluoromisonidazole is directly related to the degree of hypoxia. In contrast, in the work by Kavanagh et al. (27) no relationship was found between pO<sub>2</sub> measurements and the binding of misonidazole in murine tumours.

The aim of the present study was to compare PET measurements of tumour hypoxia with pO<sub>2</sub> electrode measurements using an Eppendorf Histogram in the same experimental mice tumours subjected to carbogen and normal air. Furthermore, we wanted to examine the relationship between the hypoxia measurements and the volume of the tumours to address the importance of tumour volume for the hypoxia assessment. The heterogeneity in the radioactive labelling in the tumours was examined using autoradiography.

## MATERIAL AND METHODS

### *Animals and tumour model*

CDF1 female mice at 12–16 weeks of age and weighing approximately 25 g with C3H mouse mammary carcinomas transplanted on their backs were used (28). The study presents results from PET and pO<sub>2</sub> measurements in a total of 45 animals; of these the PET measurements on 26 tumours were presented in our methodological study (22). In addition, autoradiography results on four separate tumours are presented. All experiments were performed in accordance with institutionally and nationally approved guidelines for animal welfare.

### *Experimental set-up*

Tumour volume was calculated by measuring the three orthogonal tumour diameters D1, D2 and D3 and using the formula,  $\text{Volume} = \pi/6 \times D1 \times D2 \times D3$ . The PET measurement was then performed followed by the pO<sub>2</sub> measurements. During the PET examinations and pO<sub>2</sub> measurements, the animals were breathing either normal atmospheric air (control animals) or were gassed with either normal air (21% oxygen) or carbogen (95% oxygen, 5% CO<sub>2</sub>) gas at a flow rate of 2.5 l/min delivered through

a custom-built nozzle placed in front of the jig (29). The gassing procedure was started at least 5 min prior to start of measurement and continued throughout the PET and pO<sub>2</sub> measurements.

### *PET examination*

The experimental set-up was as previously described (22). In short, mice were anaesthetized with 0.3 ml mebumal (4.76 mg/ml saline) injected intraperitoneally, and had a venflon catheter placed as a bladder catheter flushed with saline at regular intervals to minimize bladder radioactivity accumulation (in three of the animals a bladder catheter was not used). Animals were restrained in plastic jigs and had an intravenous (i.v.) line inserted into the tail vein, flushed with heparin saline. Scanning was performed when the animals had recovered from the anaesthetic and had been fasting for at least 3 h. Six mice were placed in a custom-built, plastic device and placed in the gantry of a Siemens ECAT EXACT HR (961) scanner. The PET scanning started with a 15-min transmission scan, used for attenuation correction. Then 0.7–3.2 MBq [<sup>18</sup>F]FMISO with a radiochemical purity of 100% (22) was administered i.v. and emission scanning performed for 5 h. Scanning was performed with 47 axial slices each of 3.1 mm in the 15-cm field of view, yielding radioactivity concentration measurements in voxels of 3.1 × 2.4 × 2.4 mm<sup>3</sup>. Data were reconstructed by using a Ramp filter with a cut-off frequency of 0.5, resulting in an almost uniform resolution with a full width at half maximum (FWHM) of 4.5 mm. Data were recorded as integrated mean values of the radioactivity in each of the time frames and radioactivity decay corrected to the start of the tracer injection.

### *PET image analysis*

Visual analysis of the data was performed in images of transaxial slices, as previously described (22). In short, the tumours were most readily identified in images from the last part of the scanning procedure. Regions of interest (ROIs) were defined in the tumours and in reference tissue, which was selected five slices (15.5 mm) cranially to the heart level in order to avoid inclusion of radioactivity in the liver, kidney and bladder. The ROIs were defined by identifying the pixel with the maximum radioactivity concentration and including pixels with activities equal to or higher than 75% of this maximum value (75% isocontour tool with ECAT software). The x and y diameters of the ROIs were measured with the ECAT7 software and approximated to a sphere with a diameter calculated as the mean value of x and y. Owing to limited resolution of the PET-scanner, the radioactivity concentrations in small objects appear lower than they really are—known as the partial volume effect. The factor by which this radioactivity is reduced is called a recovery coefficient. To account for the partial volume effect, recovery coefficients were calculated for spheres of various diameters and used for

approximated correction for the radioactivity of the ROIs (22). Time activity curves for both tumour and reference ROI were reported as the corrected average radioactivity concentration (Bq/cc tissue) for each time frame. The ratio of radioactivity between tumour ROI and reference tissue ROI was calculated. As shown in our previous work, the ratio typically increased for the animals until about 200 min after the tracer injection after which a 'quasi' steady state was reached, and the PET ratios (PET hypoxia ratios) are calculated as means of the ratios from 225 to 300 min after tracer injection.

#### *pO<sub>2</sub> measurements*

The pO<sub>2</sub> measurements were performed within about 12 h after the PET procedure, but usually within the first few hours. Measurements of tumour pO<sub>2</sub> were made using a computerized fine-needle (0.35 mm diameter), polarographic, oxygen-sensitive electrode probe (pO<sub>2</sub> Histogram, Eppendorf, Hamburg, Germany). The exact details have been described elsewhere (30, 31). In short, the skin covering the tumour was penetrated with a fine-gauge needle before the oxygen probe was inserted approximately 1 mm into the tumour. From there, the probe was automatically moved through the tumour in a stepwise pattern, with a forward step of 0.7 mm followed by a backward step of 0.3 mm to avoid tissue compression of the oxygen electrode tip, thus measuring with a net step length of 0.4 mm in a measuring track. The length of the track was determined by the tumour size and the number of parallel tracks per tumour ranged between 3 and 8 and the number of values ranged between 39 and 117, with the highest numbers seen in the larger tumours. The pO<sub>2</sub> measurements were corrected for tumour temperature, determined by inserting a thermocouple needle probe (Ellab Instruments, Copenhagen, Denmark) into the tumour after the pO<sub>2</sub> measurement. Measurements from tracks with negative values were included provided these values were between 0 and -2.0 mmHg, otherwise those tracks were rejected from the data material. Data are reported as median pO<sub>2</sub> and % ≤ 2.5 mmHg. These cut points are likely to reflect radiobiological hypoxia (32) and, furthermore, have shown to be indicators of poorer disease and overall survival of soft tissue sarcomas and prognostic of locoregional control of head and neck cancer after treatment in our previous clinical studies (12, 33).

#### *Autoradiography*

In four mice an autoradiography experiment was carried out. The experimental set-up was similar to the PET and pO<sub>2</sub>, but without using anaesthetics and bladder catheters. Two animals were breathing normal air and two animals were breathing carbogen. The animals had a mean of 2.86 (2.72–3.15) MBq [<sup>18</sup>F]FMISO injected i.v., and 120 min after the tracer administration, the animals were killed and the tumours quickly removed. The tumours were rapidly

frozen in isopentane placed on dry ice, and after embedding in Tissue-Tek, they were cut on a microtome (Jung-hans Frigocut 2800) in 20 µm-thick slices. Randomly selected slices were placed in contact with an imaging plate (Fuji BAS TR2025) for 2–3 h. The spatial distribution of <sup>18</sup>F-radioactivity from tumour slices was recorded autoradiographically with a phosphoimaging device (Fujifilm BAS-5000, Fuji Photo Film Co. Ltd., Japan). The resolution (i.e. pixel size) of the images was 25 × 25 µm.

## RESULTS

### *PET examinations and pO<sub>2</sub> measurements*

Eight PET experiments were done with a total of 45 tumour-bearing animals. In three of the tumours examined, the activity could not be corrected for partial volume effect due to a very low and uncertain recovery coefficient. Measurements from these three tumours were not included in the material. In two mice, both treated with carbogen, the tumours could not be identified by the visual PET image analysis; this was not due to a mistaken injection of saline, since both animals could be visually identified on the images. One additional tumour could not be discriminated because of spillover effects from the mouse bladder. This left a total of 39 tumours to be evaluated.

### *Tumour volume and hypoxia*

No significant differences were found between the groups breathing either normal air (controls) or gassed with normal air with respect to the PET hypoxia ratios and the pO<sub>2</sub> measurements (see Table 1). In Fig. 1 significant correlations between the median pO<sub>2</sub> and the tumour volume ( $r = -0.74$ , Spearman's rank correlation test,  $p < 0.01$ ), and the percentage of pO<sub>2</sub> measurements less than or equal to 2.5 mmHg and tumour volume ( $r = 0.64$ , Spearman's rank correlation test,  $p < 0.01$ ) are shown in these animals. No significant correlation was seen between the PET hypoxia ratios and the tumour volumes (Fig. 2).

### *Influence of carbogen breathing*

The Table shows the PET and pO<sub>2</sub> measurements for the animals gassed with either carbogen or normal air. In this part of the study, a more comparable range of tumour volumes was used than that for the animals breathing normal air. There was a significant difference between the PET ratios from the carbogen and normal air groups as previously reported (22). The percentage of pO<sub>2</sub> values less than or equal to 2.5 showed a significant difference for the carbogen and normal air groups, whereas the median pO<sub>2</sub> did not reach statistical significance ( $p = 0.12$ ).

### *Relationship between PET and pO<sub>2</sub> measurements*

In Fig. 3 we compared the PET hypoxia ratios with the tumour pO<sub>2</sub> measurements for the animals gassed either with carbogen or normal air,  $n = 26$ . The tumour vol-

Table 1

Tumour volumes, PET hypoxia ratios and pO<sub>2</sub> measurements in 39 C3H mammary carcinomas

|   | Volume (mm <sup>3</sup> )  | PET hypoxia ratio           | Median pO <sub>2</sub> (mmHg) | pO <sub>2</sub> ≤ 2.5 mmHg (%) |
|---|----------------------------|-----------------------------|-------------------------------|--------------------------------|
| Normal air (n = 13)   | 1037 (188–1451)            | 7.6 (3.0–12.6)              | 1 (0–21)                      | 77 (9–99)                      |
| Gassed with normal air (n = 13)                                 | 622 <sup>1</sup> (311–791) | 7.0 <sup>1</sup> (2.9–11.8) | 4 <sup>1</sup> (1–29)         | 32 <sup>1</sup> (4–84)         |
| Gassed with carbogen (95% oxygen, 5% CO <sub>2</sub> ) (n = 13) | 645 <sup>2</sup> (403–791) | 2.3 <sup>3</sup> (0.7–5.1)  | 9 <sup>4</sup> (2–78)         | 11 <sup>5</sup> (0–58)         |

Data are reported as median and range values, all statistical tests were Mann–Whitney U-tests. NS indicates  $p > 0.05$ .

<sup>1</sup> NS: when comparing animals breathing normal air with those gassed with normal air.

<sup>2</sup> NS: tumour volume compared for carbogen and air gassed.

<sup>3</sup>  $p < 0.01$ , PET ratio compared for carbogen and air gassed.

<sup>4</sup>  $p = 0.12$ , median pO<sub>2</sub>, carbogen and air gassed.

<sup>5</sup>  $p = 0.03$ , pO<sub>2</sub> ≤ 2.5 mmHg, compared for carbogen and air gassed.

umes from the two groups of animals were comparable. The median pO<sub>2</sub> and the PET hypoxia ratios were compared and there was no significant correlation ( $p > 0.05$ , Spearman's rank correlation test). For low median pO<sub>2</sub> values there was a wide range of PET hypoxia ratios,

whereas for higher median pO<sub>2</sub> values the spread of the PET hypoxia ratios was less. The percentage of values below or equal to 2.5 mmHg was compared with the PET hypoxia ratios, but again no correlation was found (Fig. 3). The three carbogen-treated tumours that demonstrated a high percentage of values below or equal to 2.5 mmHg combined with low PET ratio values, all had large tumour volumes. In Fig. 4, the PET hypoxia ratios are plotted against the pO<sub>2</sub> measurements for the tumours on the animals breathing normal air or gassed with normal air (Table 1). In this figure, the volumes of the tumours were divided into tertiles. For the largest tumours there was a trend towards showing more hypoxic pO<sub>2</sub> measurements and at the same time a wide range of PET ratios.

#### Autoradiography data

The autoradiography data are shown in Fig. 5 for four tumours: two with a small volume of 220 mm<sup>3</sup> and two

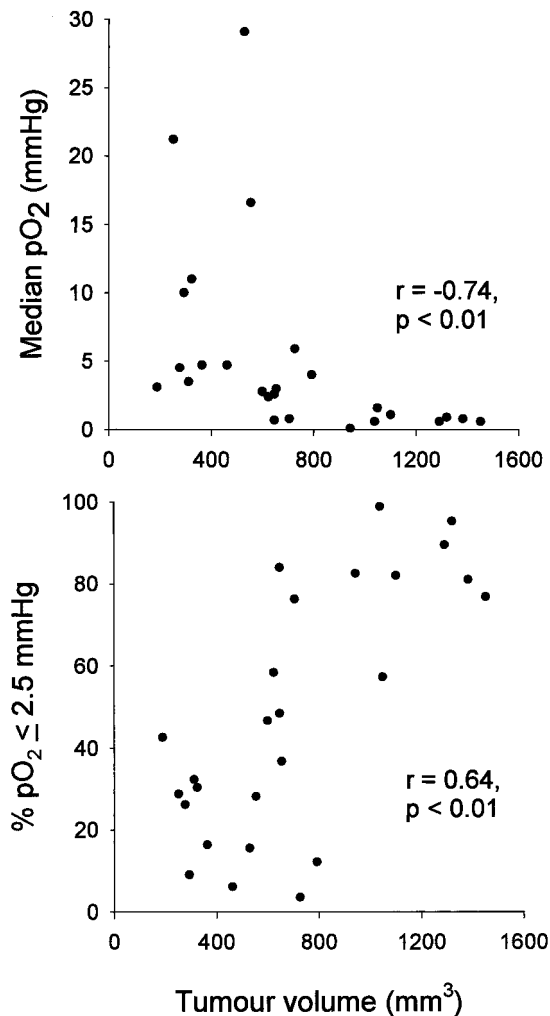


Fig. 1. Relationship between pO<sub>2</sub> measurements and tumour volume for animals breathing either normal air or gassed with normal air (n = 26).

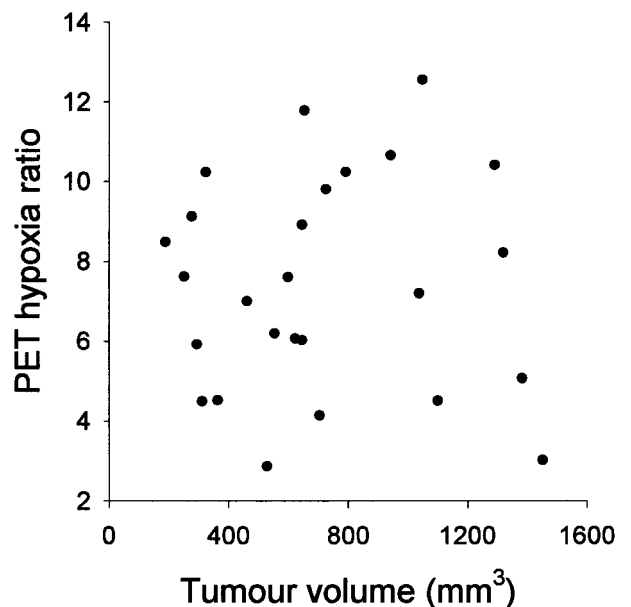


Fig. 2. PET hypoxia ratios are plotted against tumour volumes for animals breathing either normal air or gassed with normal air (n = 26).

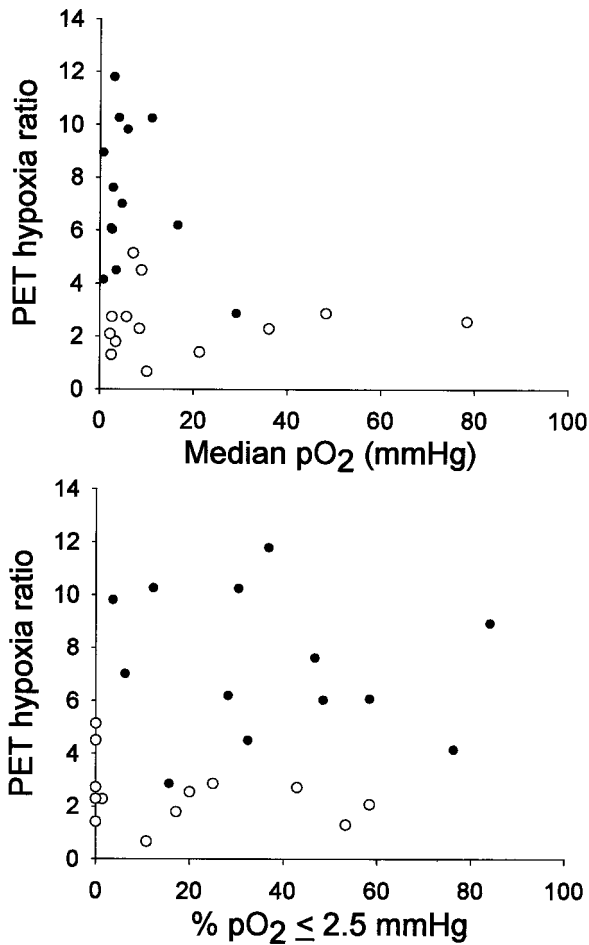


Fig. 3. PET hypoxia ratios plotted against the  $pO_2$  measurements in tumours on mice gassed with either carbogen (○) or normal air (●),  $n = 26$ .

with a volume of approximately  $550 \text{ mm}^3$ . In the normal air-breathing mice, tumours were labelled more with the  $[^{18}\text{F}]\text{FMISO}$  than the carbogen-treated tumours. In the small tumours, the labelling was relatively uniformly distributed throughout the tumour tissue for the control, whereas in the carbogen-treated tumour a central uptake of the tracer dominated. For the larger tumours, there was a central sparing concerning the uptake of tracer, most clearly seen for the carbogen-treated tumour but also evident in the tumour of the control animal.

## DISCUSSION

### Hypoxia measurements and volume

Significant correlations between  $pO_2$  measurements and tumour volume are shown in Fig. 1. These correlations were in good agreement with the work by Khalil et al. (13), where a correlation between the volume of C3H mammary tumours and the percentage of  $pO_2$  measurements below or equal to  $5.0 \text{ mmHg}$  was shown. Further-

more, Khalil et al. showed that when a correction for necrosis was taken into account, this correlation disappeared. The conclusion of that study was that if necrosis was present in the tumours, the  $pO_2$  measurements could result in an overestimation of hypoxia. In contrast, the study by Milross et al. (34) confirmed the dependence of hypoxia on the tumour volume, but did not find that correction of  $pO_2$  for necrosis rejected the correlation. De Jaeger et al. (35) found that differences in oxygenation in various tumours tended to persist as they grew larger. Thus, the decrease in oxygenation measured with oxygen electrodes could be because of measurements obtained in necrotic tissue, although this hypothesis remains to be further investigated.

The PET measurements for the animals either gassed or breathing normal air were plotted against tumour volume in Fig. 2. No correlation between the parameters was found, indicating that hypoxia assessed by this PET method was independent of tumour size. Khalil et al. (36) found that the necrotic fraction in C3H mammary carcinomas implanted on the foot increased with the volume of the tumour, whereas no difference in hypoxia estimated by the radiobiological hypoxic fraction for foot tumours in the size range  $50\text{--}700 \text{ mm}^3$  was found. Since the *in vivo* binding of the hypoxia tracer should not occur in necrotic tissue, the results of our PET assay applied to C3H mammary carcinomas implanted on the backs of the mice supported the conclusion that no increase in hypoxic fraction is seen with increasing tumour size.

### Relationship of PET and $pO_2$ measurements

Comparison of the PET measurements with the  $pO_2$  measurements for the animals gassed with either carbogen or

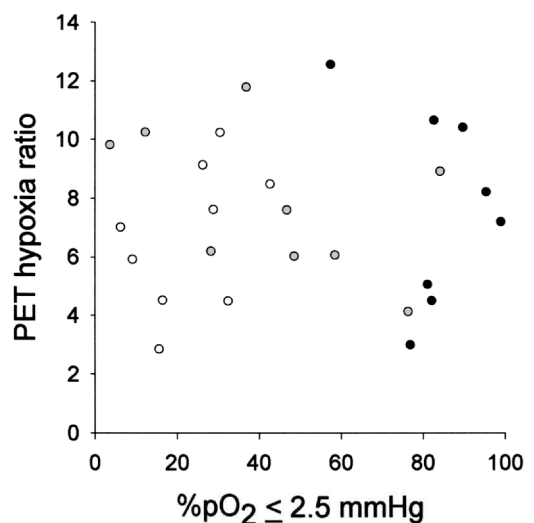


Fig. 4. PET hypoxia ratio plotted against  $pO_2$  measurements for animals breathing either normal air or gassed with normal air ( $n = 26$ ). Open symbols represent the smallest tumours, grey symbols the intermediate tumour size and the black symbols represent the largest tumours.

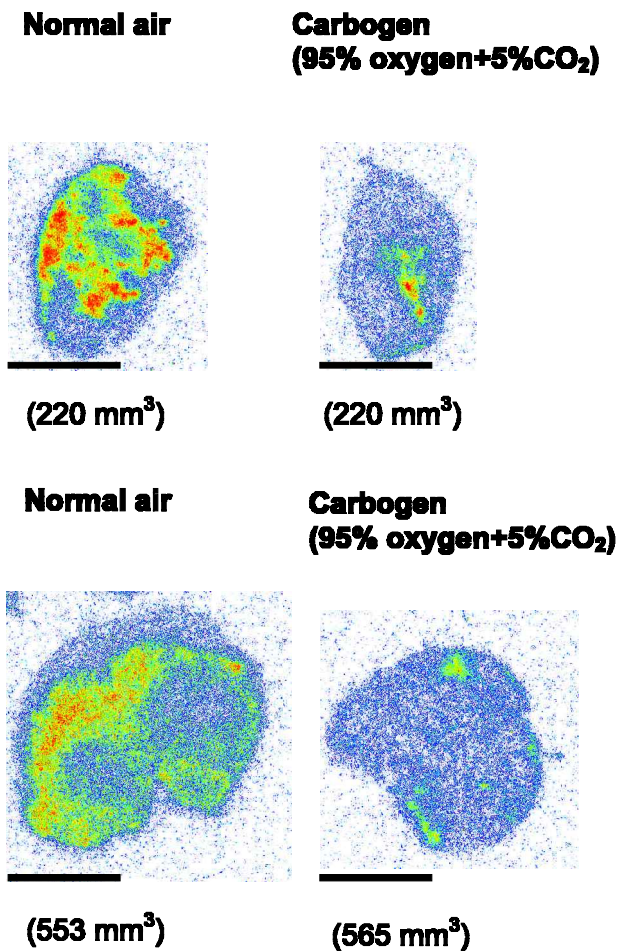


Fig. 5. Autoradiography images of <sup>18</sup>F-FMISO labelling (resolution 25 × 25 μm) of four C3H mammary carcinomas, two gassed with carbogen and two breathing normal air, volume matched as shown on the Figure. The blue area represents the lowest and the red area the highest radioactivity concentration. The black bars show 0.5 cm.

normal air (Table 1) and with comparable tumour volumes showed no correlation between the two methods (Fig. 3). The PET data analysis is based on selecting an area in the tumour labelled with the tracer and reporting an average radioactivity of that area. Heterogeneity in the distribution of the tracer will influence the mean radioactivity concentration. However, the outlining of the ROIs was based on the most hypoxic area in the tumours, thus making it reasonable to compare the PET measurements with both the median pO<sub>2</sub> measurements and the percentages of measurements below 2.5 mmHg. To a large extent, the median pO<sub>2</sub> and the PET-assessed hypoxia fit with high PET ratios corresponding to low median pO<sub>2</sub> values, but for PET ratios below 4 there is a large variability in the median oxygen tension. Four of the tumours had low median oxygen tensions (2.2–3.4 mmHg) and low PET

ratios (1.3–2.7). Those four tumours also were quite large (545–791 mm<sup>3</sup>). Plotting the PET data against tumour volumes (Fig. 2) showed that with large volumes the PET ratios seemed to decrease. Comparing this with the plot of PET-assessed hypoxia against the median oxygen tension in the tumours may offer an explanation for the large variability discussed above. The reason for the PET ratios decreasing as the volume of the tumour increases is not clear. If the analysis of the ROIs on which the PET analysis is based included pixels with lower tracer accumulation, these would tend to 'dilute' the overall average tracer uptake, thereby underestimating the hypoxia. However, our use of the 75% isocontour for determination of ROIs should have overcome this issue. A more likely explanation for the discrepancy between the median pO<sub>2</sub> and the PET examination in the large tumours could be the simple fact that the pO<sub>2</sub> measurements tend to overestimate the degree of hypoxia in these large tumours, because some of the measurements are actually done in necrotic tissue. Interestingly, in a clinical study, the labelling of tumours of the cervix with pimonidazole was compared to the assessment of oxygen status with the Eppendorf method and no direct correlation between the assays was found (37). Nordmark et al. also demonstrated a low pimonidazole labelling for some of the tumours that had a relatively high fraction of hypoxic measurements with the Eppendorf method.

In the work by Kavanagh et al. (27), a comparison between the uptake of [<sup>3</sup>H]misonidazole and pO<sub>2</sub> measurements in different murine tumours showed no correlation. However, the assays were not carried out in the same tumours, which weakens the conclusion. Jenkins et al. (24) studied the 2-nitroimidazole hypoxia marker EF5 and oxygen assessment with pO<sub>2</sub> measurements in rodent tumours and found that the pO<sub>2</sub> measurements tended to overestimate the tumour hypoxia, whereas the EF5 assay tended to underestimate tumour hypoxia because of minimal binding in pre-necrotic areas. Both methods are thus biased by necrosis in the tumour. One suggestion for the low labelling with EF5 proposed by the authors was the possibility of EF5 delivery problems to ischaemic regions. Other hypoxia markers have been developed, among them the Cu-ATSM. Lewis et al. showed this tracer to be highly selective for hypoxic cells (38) and recently it was shown that the accumulation of this tracer assessed by autoradiography in a rat gliosarcoma model correlated with invasive oxygen measurements (39).

Recently, Raleigh et al. (23) showed that there is a significant correlation between Eppendorf pO<sub>2</sub> measurements and both binding of pimonidazole and the radiobiological hypoxic fraction in the C3H mammary carcinoma when groups of tumours were examined under different oxygen conditions. In the present study we examined the correlation between two hypoxia-estimating assays using

the same murine tumour model but at different sizes and implanted at another site. The necrotic fraction in the C3H mammary carcinoma differs substantially when different sizes are examined (13) and this fact works against finding a correlation between the assays in our study (Figs. 3 and 4). In the work by Piert et al. (26, 40), it was found that, regardless of ventilation conditions, a significant inverse relationship existed between mean  $pO_2$  measurements by the Eppendorf electrode and the standardized uptake value of [ $^{18}F$ ]FMISO evaluated by PET examination in liver tissue. The authors concluded that [ $^{18}F$ ]FMISO PET allowed for in vivo quantification of pig liver hypoxia. That study also reported histological findings, and parenchymal cell necrosis was found in the tissue subjected to impaired arterial blood delivery. However, this was not directly compared with the  $pO_2$  and PET measurements.

#### *Influence of carbogen breathing*

In the gassing experiments, we were able significantly to discriminate between carbogen and normal air-gassed tumours by our PET assay as well as with one  $pO_2$  parameter, the percentage of values less than or equal to 2.5 mmHg. Using median  $pO_2$ , no significant discrimination between the two groups was obtained. As discussed previously, in larger tumours the  $pO_2$  measurements can tend to over-report hypoxia owing to necrosis. From our PET results, it seems that we may have a more sensitive assay for hypoxia in the tumour sizes examined in the gassing experiments. To further illustrate the tracer binding in the tumours compared to both tumour size and treatment, the autoradiography experiment shown in Fig. 5 was carried out. As mentioned in the Results section, the labelling was quite heterogeneous, and the distribution of the tracer seemed to depend on both treatment and tumour size. For the larger tumours, large areas with no labelling were present. The resolution of the autoradiography experiment was excellent in comparison to the actual sizes of the tumours, and the autoradiography method combined with consecutive histological sections analysed for necrotic fraction will provide further information regarding labelling tumours with hypoxia tracers and estimating necrosis. For clinical purposes, it is important to show heterogeneity of the tracer uptake, as this might give truer reporting of hypoxic areas, and for larger tumour volumes (i.e. human tumours) it should be possible to do pixel to pixel analysis of the tracer uptake as measured with PET scanning. However, in this experimental study where the ROIs are very small compared to the resolution of the PET scanner, it serves no purpose to pursue this issue.

We presented two different methods for detection of hypoxia—a method based on an invasive measurement and a method based on non-invasive metabolic imaging. Both are capable of discriminating between a high and

low degree of hypoxia in these experimental tumours, but they do not correlate. This present study therefore does not offer a specific amount of [ $^{18}F$ ]FMISO accumulation as indicative of hypoxia. Rasey et al. (41) compared FMISO tumour to blood ratios with the hypoxic fraction measured with the paired survival curve assay, and found that those ratios might be predictive for hypoxic fraction. Given the technical difficulties in performing the PET experiments in such small animals with small tumours, this study should be continued in human tumours in order to further evaluate whether a correlation between the methods can be found. From former studies we know that  $pO_2$  measurements are predictive of treatment outcome in certain solid tumours in patients (9, 10, 33). This has yet to be shown for the [ $^{18}F$ ]FMISO PET scanning. However, our autoradiography study supported the finding that the [ $^{18}F$ ]FMISO clearly binds in lower amounts in tumours subjected to a higher content of oxygen because of carbogen gassing.

#### CONCLUSION

In this study we found that invasive  $pO_2$  measurements in C3H mammary carcinomas implanted on the backs of CDF1 mice correlated with the volumes of the tumours. The correlation of the  $pO_2$  measurements with volume was suggested to relate to the fact that necrosis increases with tumour volume and that the electrode measurements could have been performed partly in necrotic tissue. PET-assessed hypoxia in the same tumours did not correlate with tumour volume. The PET assay relies on binding of [ $^{18}F$ ]FMISO in cells, a binding that only takes place in viable hypoxic cells and should not label necrosis in the tumours. The experimental tumour used in this study has been shown to demonstrate a constant radiobiologically determined hypoxic fraction in tumours ranging in size from 50 to 700 mm<sup>3</sup>. This supported the finding in the present study. With the modification of oxygen content by carbogen breathing, the labelling with [ $^{18}F$ ]FMISO was significantly changed, which implied that the tracer labelled hypoxic cells. This was further supported by the autoradiography findings. The  $pO_2$  measurements did not correlate with the PET examinations, but were able significantly to distinguish between carbogen-treated tumours and the normal air-treated tumours. As the PET assay offered a limited resolution compared to the tumour size examined, future examinations comparing the two assays should be performed in human tumours.

#### ACKNOWLEDGEMENTS

This study was supported by a grant from the Danish Cancer Society. We express our thanks to I. M. Johansen, D. Grand and M. H. Simonsen for excellent technical assistance. We also thank Päivi Marjamäki, FM, for excellent assistance with the autoradiography studies.

## REFERENCES

- Moulder JE, Rockwell S. Hypoxic fractions of solid tumors: experimental techniques, methods of analysis, and a survey of existing data. *Int J Radiat Oncol Biol Phys* 1984; 10: 695–712.
- Grau C, Overgaard J. Effect of cancer chemotherapy on the hypoxic fraction of a solid tumor measured using a local tumor control assay. *Radiother Oncol* 1988; 13: 301–9.
- Grau C, Horsman MR, Overgaard J. Improving the radiation response in a C3H mouse mammary carcinoma by normobaric oxygen or carbogen breathing. *Int J Radiat Oncol Biol Phys* 1992; 22: 415–9.
- Overgaard J, Horsman MR. Modification of hypoxia-induced radioresistance in tumors by the use of oxygen and sensitizers. *Semin Radiat Oncol* 1996; 6: 10–21.
- Sutherland RM, Ausserer WA, Murphy BJ, Laderoute KR. Tumour hypoxia and heterogeneity: challenges and opportunities for the future. *Semin Radiat Oncol* 1996; 6: 59–70.
- Giaccia AJ. Hypoxic stress proteins: survival of the Fittest. *Semin Radiat Oncol* 1996; 6: 46–58.
- Graeber TG, Osmanian C, Jacks T, et al. Hypoxia-mediated selection of cells with diminished apoptotic potential in solid tumours. *Nature* 1996; 379: 88–91.
- Dachs GU, Tozer GM. Hypoxia modulated gene expression: angiogenesis, metastasis and therapeutic exploitation. *Eur J Cancer* 2000; 36: 1649–60.
- Kolstad P. Intercapillary distance, oxygen tension and local recurrence in cervix cancer. *Scand J Clin Lab Invest* 1968; 106 (Suppl): 145–57.
- Nordsmark M, Overgaard M, Overgaard J. Pretreatment oxygenation predicts radiation response in advanced squamous cell carcinoma of the head and neck. *Radiother Oncol* 1996; 41: 31–9.
- Hockel M, Schlenger K, Aral B, Mitze M, Schaffer U, Vaupel P. Association between tumor hypoxia and malignant progression in advanced cancer of the uterine cervix. *Cancer Res* 1996; 56: 4509–15.
- Nordsmark M, Alsnér J, Keller J, et al. Hypoxia in human soft tissue sarcomas: adverse impact on survival and no association with p53 mutations. *Br J Cancer* 2001; 84: 1070–5.
- Khalil AA, Horsman MR, Overgaard J. The importance of determining necrotic fraction when studying the effect of tumour volume on tissue oxygenation. *Acta Oncol* 1995; 34: 297–300.
- Brown JM, Yu NY, Cory MJ, Bicknell RB, Taylor DL. In vivo evaluation of the radiosensitizing and cytotoxic properties of newly synthesized electron-affinic drugs. *Br J Cancer* 1978; 37 (Suppl): 206–11.
- Chapman JD, Franko AJ, Sharplin J. A marker for hypoxic cells in tumours with potential clinical applicability. *Br J Cancer* 1981; 43: 546–50.
- Hirst DG, Hazlehurst JL, Brown JM. Changes in misonidazole binding with hypoxic fraction in mouse tumors. *Int J Radiat Oncol Biol Phys* 1985; 11: 1349–55.
- Raleigh JA, Miller GG, Franko AJ, Koch CJ, Fuciarelli AF, Kelly DA. Fluorescence immunohistochemical detection of hypoxic cells in spheroids and tumours. *Br J Cancer* 1987; 56: 395–400.
- Urtasun RC, Chapman JD, Raleigh JA, Franko AJ, Koch CJ. Binding of 3H-misonidazole to solid human tumors as a measure of tumor hypoxia. *Int J Radiat Oncol Biol Phys* 1986; 12: 1263–7.
- Koh WJ, Rasey JS, Evans ML, et al. Imaging of hypoxia in human tumors with [F-18]fluoromisonidazole. *Int J Radiat Oncol Biol Phys* 1992; 22: 199–212.
- Koh WJ, Bergman KS, Rasey JS, et al. Evaluation of oxygenation status during fractionated radiotherapy in human non-small cell lung cancers using [F-18]fluoromisonidazole positron emission tomography. *Int J Radiat Oncol Biol Phys* 1995; 33: 391–8.
- Rasey JS, Koh WJ, Evans ML, et al. Quantifying regional hypoxia in human tumors with positron emission tomography of [18F]fluoromisonidazole: a pretherapy study of 37 patients. *Int J Radiat Oncol Biol Phys* 1996; 36: 417–28.
- Bentzen L, Keiding S, Horsman MR, Falborg L, Hansen SB, Overgaard J. Feasibility of detecting hypoxia in experimental mouse tumours with 18F-fluorinated tracers and positron emission tomography—a study evaluating [18F]fluoromisonidazole and [18F]Fluoro-2-deoxy-D-glucose. *Acta Oncol* 2000; 39: 629–37.
- Raleigh JA, Chou SC, Arteel GE, Horsman MR. Comparisons among pimonidazole binding, oxygen electrode measurements, and radiation response in C3H mouse tumors. *Radiat Res* 1999; 151: 580–9.
- Jenkins WT, Evans SM, Koch CJ. Hypoxia and necrosis in rat 9L glioma and Morris 7777 hepatoma tumors: comparative measurements using EF5 binding and the Eppendorf needle electrode. *Int J Radiat Oncol Biol Phys* 2000; 46: 1005–17.
- Evans SM, Hahn S, Pook DR, et al. Detection of hypoxia in human squamous cell carcinoma by EF5 binding. *Cancer Res* 2000; 60: 2018–24.
- Piert M, Machulla H, Becker G, et al. Introducing fluorine-18 fluoromisonidazole positron emission tomography for the localisation and quantification of pig liver hypoxia. *Eur J Nucl Med* 1999; 26: 95–109.
- Kavanagh MC, Sun A, Hu Q, Hill RP. Comparing techniques of measuring tumor hypoxia in different murine tumors: Eppendorf pO<sub>2</sub> histogram, [3H]misonidazole binding and paired survival assay. *Radiat Res* 1996; 145: 491–500.
- Overgaard J. Simultaneous and sequential hyperthermia and radiation treatment of an experimental tumor and its surrounding normal tissue in vivo. *Int J Radiat Oncol Biol Phys* 1980; 6: 1507–17.
- Grau C, Horsman MR, Overgaard J. Influence of carboxy-hemoglobin level on tumor growth, blood flow, and radiation response in an experimental model. *Int J Radiat Oncol Biol Phys* 1992; 22: 421–4.
- Kallinowski F, Zander R, Hoeckel M, Vaupel P. Tumor tissue oxygenation as evaluated by computerized-pO<sub>2</sub>-histography. *Int J Radiat Oncol Biol Phys* 1990; 19: 953–61.
- Horsman MR, Khalil AA, Nordsmark M, Grau C, Overgaard J. Relationship between radiobiological hypoxia and direct estimates of tumour oxygenation in a mouse tumour model. *Radiother Oncol* 1993; 28: 69–71.
- Gray LH, Conger AD, Ebert M, Hornsey S, Scott OCA. The concentration of oxygen dissolved in tissues at the time of irradiation as a factor in radiotherapy. *Br J Radiol* 1953; 26: 638–48.
- Nordsmark M, Overgaard J. A confirmatory prognostic study on oxygenation status and loco-regional control in advanced head and neck squamous cell carcinoma treated by radiation therapy. *Radiother Oncol* 2000; 57: 39–43.
- Milross CG, Tucker SL, Mason KA, Hunter NR, Peters LJ, Milas L. The effect of tumor size on necrosis and polarographically measured pO<sub>2</sub>. *Acta Oncol* 1997; 36: 183–9.
- De Jaeger K, Merlo FM, Kavanagh MC, Fyles AW, Hedley D, Hill RP. Heterogeneity of tumor oxygenation: relationship to tumor necrosis, tumor size, and metastasis. *Int J Radiat Oncol Biol Phys* 1998; 42: 717–21.
- Khalil A. A. Experimental studies on the relationship between growth and different cellular and tissue environmental

- parameters of a malignant solid tumour. Faculty of Health Sciences, University of Aarhus, 1996. Thesis.
37. Nordmark M, Loncaster J, Chou SC, et al. Invasive oxygen measurements and pimonidazole labeling in human cervix carcinoma. *Int J Radiat Oncol Biol Phys* 2001; 49: 581–6.
  38. Lewis JS, McCarthy DW, McCarthy TJ, Fujibayashi Y, Welch MJ. Evaluation of <sup>64</sup>Cu-ATSM in vitro and in vivo in a hypoxic tumor model. *J Nucl Med* 1999; 40: 177–83.
  39. Lewis JS, Sharp TL, Laforest R, Fujibayashi Y, Welch MJ. Tumor uptake of copper-diacetyl-bis(n(4)-methylthiosemicarbazone): effect of changes in tissue oxygenation. *J Nucl Med* 2001; 42: 655–61.
  40. Piert M, Machulla HJ, Becker G, Aldinger P, Winter E, Bares R. Dependency of the [<sup>18</sup>F]fluoromisonidazole uptake on oxygen delivery and tissue oxygenation in the porcine liver. *Nucl Med Biol* 2000; 27: 693–700.
  41. Rasey JS, Koh WJ, Grierson JR, Grunbaum Z, Krohn KA. Radiolabelled fluoromisonidazole as an imaging agent for tumor hypoxia. *Int J Radiat Oncol Biol Phys* 1989; 17: 985–91.